A Novel Lanthanum-based Solid Oxide Fuel Cell Electrolyte Composite with Enhanced Thermochemical Stability toward Perovskite Cathode

Supporting information

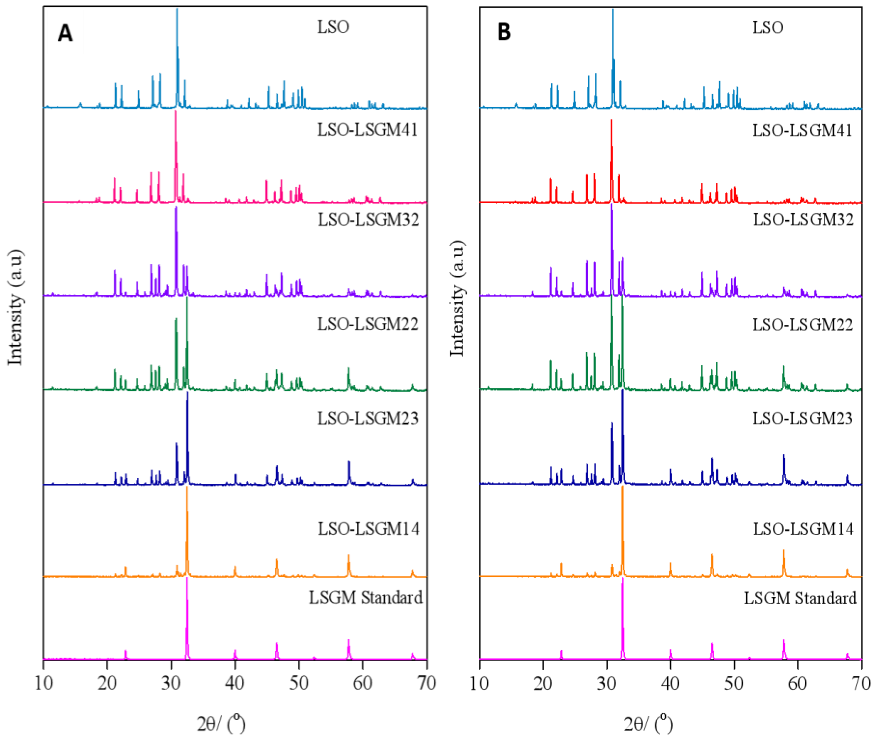

Figure S1. XRD pattern of LSO-LSGM based on LSO precursor (A) 3 g and (B) 5 g.

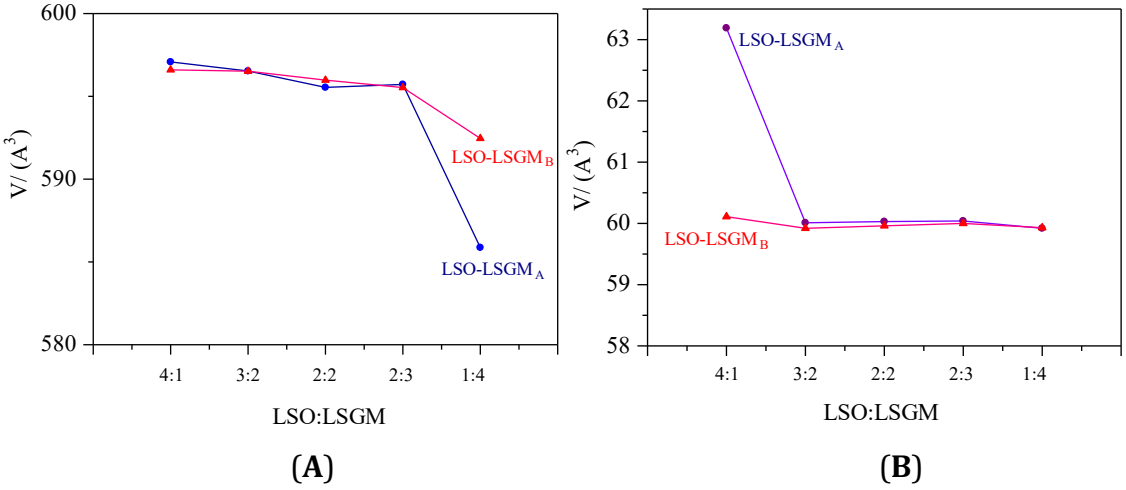

Figure S2. The change of LSO cells volume (A) and LSGM cells volume (B) at LSO-LSGM composite electrolytes with various mass ratio (4:1, 3:2, 2:2, 2:3, and 1:4).

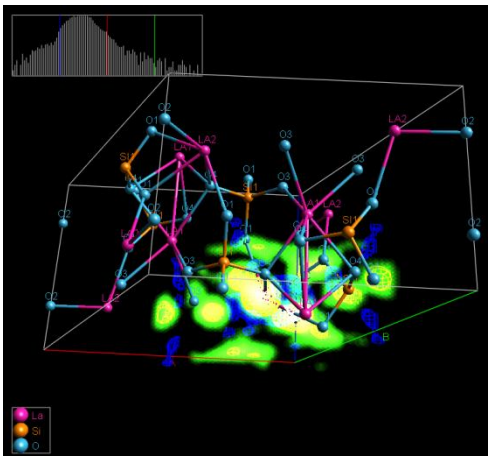

LSO_A

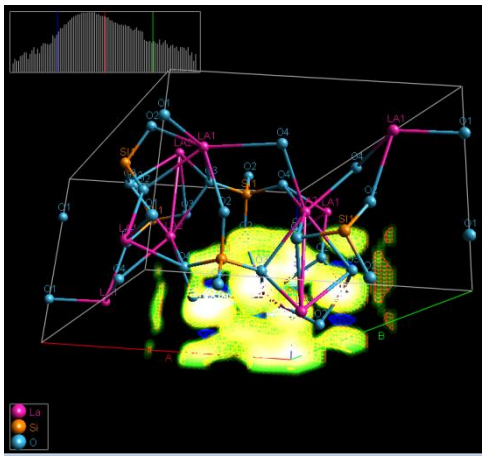

$LSO\text{-}LSGM_A41$

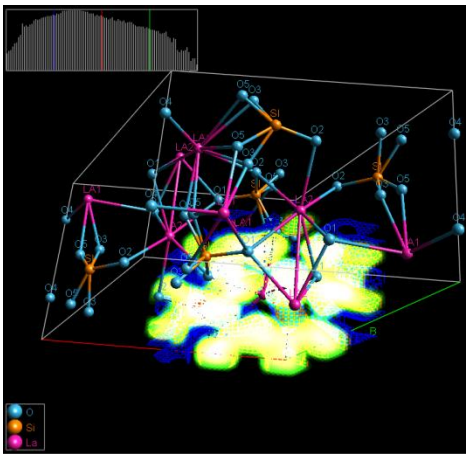

$LSO\text{-}LSGM_A32$

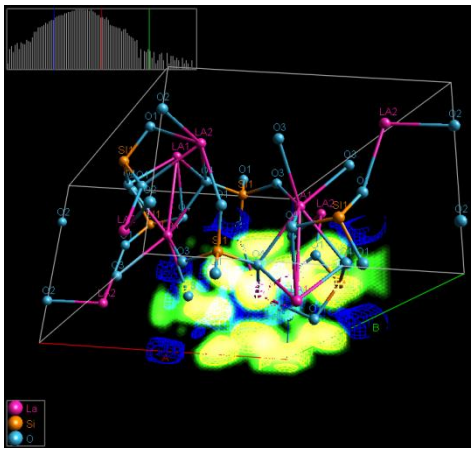

$LSO\text{-}LSGM_A22$

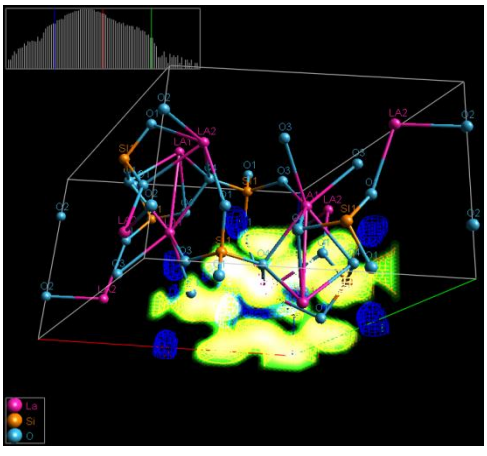

$LSO\text{-}LSGM_A23$

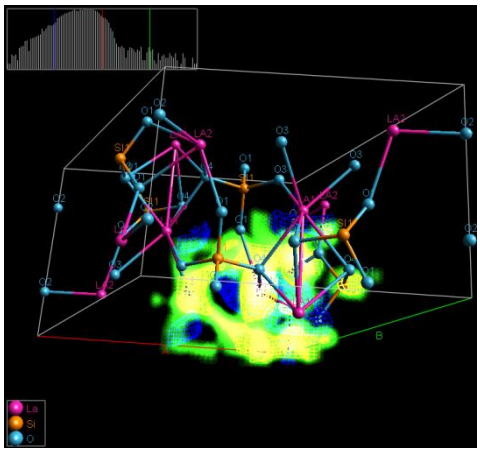

$LSO\text{-}LSGM_A14$

Figure S3. Fourier map of LSO structures in the LSO-$LSGM_A$ composite electrolytes. The green colour suggested a higher electronic density.

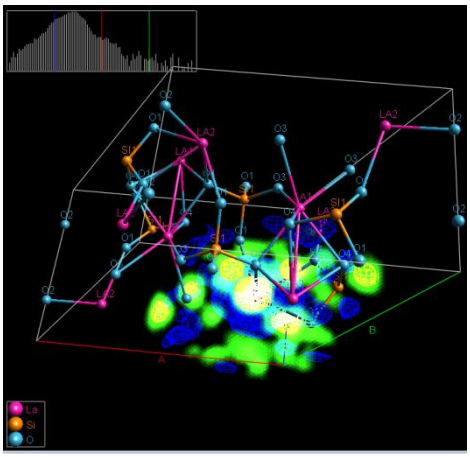

LSO_B

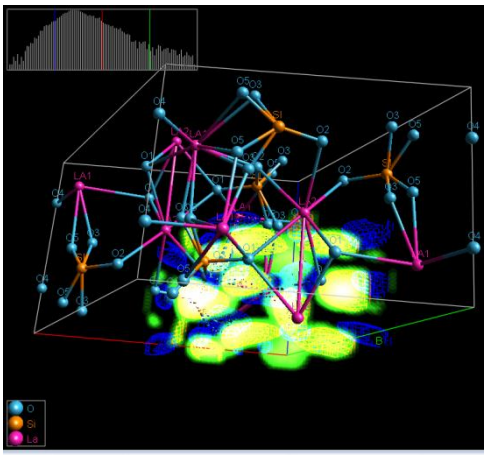

$LSO\text{-}LSGM_B41$

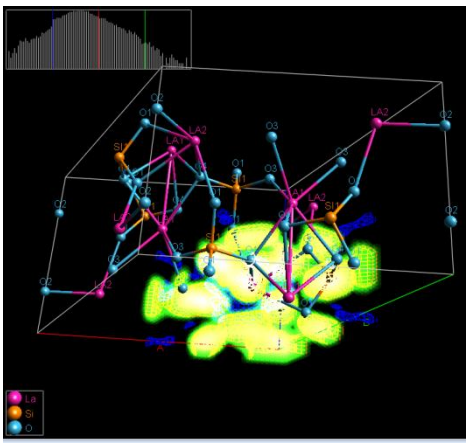

$LSO\text{-}LSGM_B32$

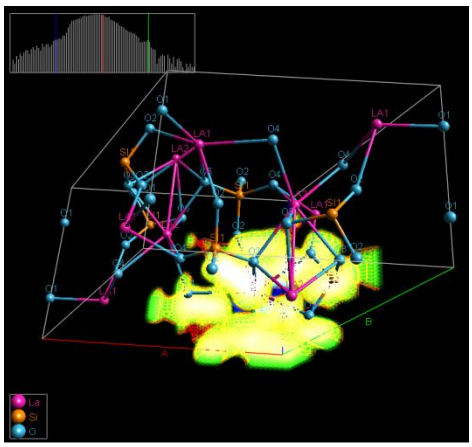

$LSO\text{-}LSGM_B22$

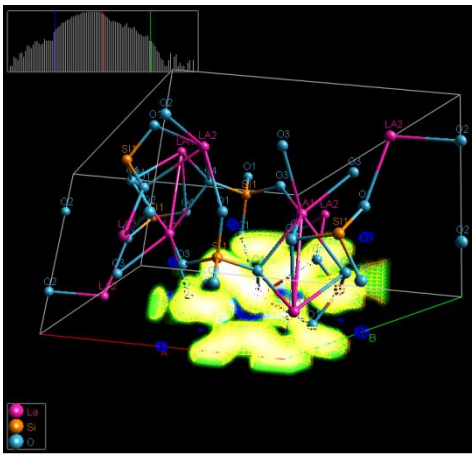

$LSO\text{-}LSGM_B23$

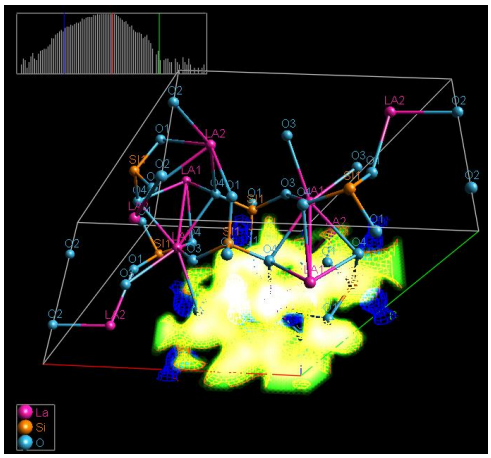

$LSO\text{-}LSGM_B14$

Figure S4. Fourier map of LSO structures in the LSO-$LSGM_B$ composite electrolytes. The green colour suggested a higher electronic density.

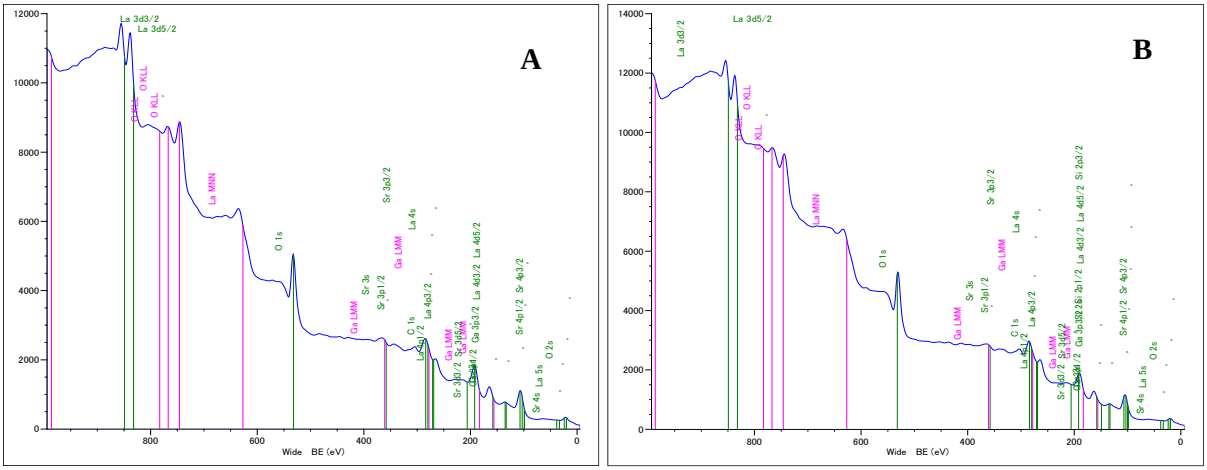

Figure S5. XPS Spectrum of LSO-LSGM$_A$ (A) and LSO-LSGM$_B$ (B)

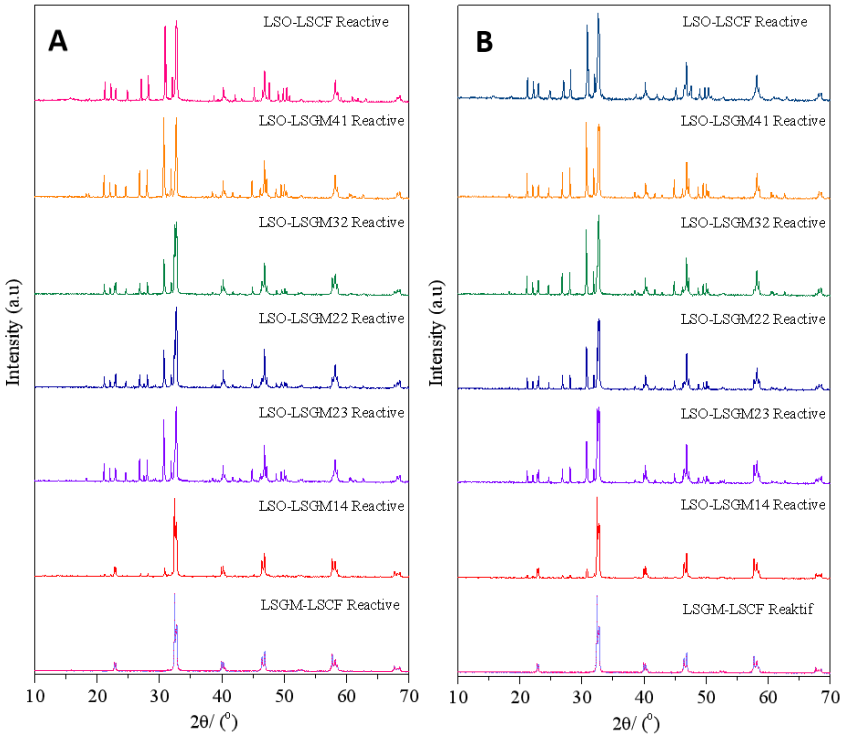

Figure S6. XRD pattern of LSO-LSGM$_A$ (A) and LSO-LSGM$_B$ (B) composite electrolytes mixed with LSCF cathode to measure the thermochemical stability.